Article

Effects of Iron Nanoparticles Addition on Bacterial Community and Phytotoxicity in Aerobic Compost of Pig Manure

Wenqing Yang [1,2,*] , Qian Zhuo [1,2], Yuanping Zhong [2], Qinghua Chen [2] and Zuliang Chen [1]

1   Fujian Provincial Key Lab of Coastal Basin Environment, Fujian Polytechnic Normal University, Fuqing 350300, China; zlchen@fjnu.edu.cn (Z.C.)
2   Engineering Research Center of Polymer Green Recycling, Ministry of Education, Fuzhou 350007, China
*   Correspondence: yangwq@fpnu.edu.cn

Abstract: In China, the treatment of pig manure for land application is an important issue. In this paper, green synthesized iron nanoparticles (G-*n*Fe) were evaluated for their effectiveness in the aerobic composting of pig manure. G-*n*Fe were evenly mixed into the compost, and the pH and oxidation-reduction potential (ORP) of the compost in the presence of G-*n*Fe both decreased. FTIR showed that G-*n*Fe promoted the formation of humus during composting. The addition of G-*n*Fe (200 mL kg^{-1}) to the compost also promoted bacterial growth, significantly increasing the colony-forming units (CFU, up to 25.6×10^4 CFU mL^{-1}) and OD600 (up to 0.634) in 5 days. Furthermore, G-*n*Fe promoted the fermentation of the pig manure, thus reducing the phytotoxicity of the compost produced. For example, the final volatile solids (VS) degradation rate and seed germination index (GI) of the compost were the highest and reached 20.8% and 0.76%, respectively. Finally, G-*n*Fe improved both the bacterial diversity and community richness of the compost. This indicated that the addition of G-*n*Fe could result in the prolonging of the acidic fermentation time during composting, leading to increased compost maturity. Overall, the beneficial impact of G-*n*Fe on compost was far greater than the potential harm to bacterial communities in the compost and perceived phytotoxicity.

Keywords: bacteriological; compost; iron nanoparticles; green synthesis; phytotoxicity

1. Introduction

Green synthesized iron nanoparticles (G-nFe) have attracted attention due to the prominent surface effects of the nanoparticles [1], and hence, G-nFe have been widely used for water and soil remediation [2,3]. For instance, Luo et al. [4,5] investigated the mechanism of both Orange II and trichloroethylene (TCE) degradation via G-*n*Fe prepared from a grape leaf extract, showing that more than 92.0% of Orange II and 93.8% of TCE was removed by G-*n*Fe based on a combination of adsorption and reduction. Thus, while G-*n*Fe have been widely proposed for practical remediation, being both cost effective and environmentally safe, the application of G-*n*Fe for enhancing the composting of pig manure has not been widely considered.

In recent decades, pollution as a consequence of livestock breeding has become a major problem for China's pig breeding industry, primarily due to the very large volumes of manure produced nationwide and increasing concern for the safety and quality of pig manure [6,7]. Due to the significant amounts of N, P, K, and other micronutrients in pig manure, which are beneficial for plant growth, it has been used as a natural organic fertilizer for millennia. However, modern pig manure can still contain a large number of heavy metals including As, Cu, Cr, Pb, and Zn, as well as a large number of other, more exotic pollutants such as pathogens and antibiotics, which can potentially damage crops and human beings who consume those crops if not managed properly [8–11]. Furthermore, the application of immature pig manure as a fertilizer is not recommended, as this can easily lead to the heat injury of seedlings and roots, and the spread of diseases and insect

pests to plants [12,13]. Thus, it is common practice to compost pig manure prior to any agricultural applications.

Pig manure composting, also known as maturation, is a process in which organic substances in the raw pig manure are transformed into other small organic substances by composting microorganisms, and other resistant organic substances such as humus are generated [14]. The high temperatures generated in composting also have the advantage of killing a large number of harmful microorganisms, where the compost microorganisms produced can also degrade some of the inorganic and organic pollutants present in the raw pig manure [15]. As an established remediation technology, very little research has been conducted recently to improve pig manure composting because of the perception that very little can be done to improve composting efficiency, with most attention being paid to the effectiveness of compost additives [16,17]. Cheap, effective, and safe compost additives can easily be introduced into existing composting practice, and thus will be readily adopted for large-scale industrial applications, with the associated expected increases in social and economic benefits. Our previous research on organic waste composting has shown that while G-*n*Fe exerted little effect on the growth of *Paracoccus* sp., it significantly promoted the growth of *Bacillus fusiformis* (BFN) [18–20] and could thus be beneficial in enhancing composting efficiency. In addition, while we also found that G-*n*Fe exerted a passivation effect on Cd in pig manure compost [21], the exact effect of G-*n*Fe on the composting process was not clear. The key knowledge gaps to be met were (1) What effect G-nFe has on composing parameters and (2) how G-nFe impacts bacterial population, diversity, and community. Exploring the mechanism of G-*n*Fe on composting will have a certain level of significance in the land application of pig manure.

This paper specifically studied the effect of G-*n*Fe on the aerobic composting process of pig manure, where the main objectives were to (1) examine the effect of G-*n*Fe on important composing parameters, e.g., hydrogen ion concentration (pH), oxidation-reduction potential (ORP), and volatile solids (VS); (2) use Fourier-transform infrared spectroscopy (FTIR) to investigate how G-*n*Fe enhances the formation of humus; (3) examine the effect of G-*n*Fe on colony-forming units (CFU) and germination index (GI); and (4) analyze bacteriological changes at the genus level, including bacterial population, diversity, and community richness, as well as the similarity and difference of bacterial communities and the variation of the abundance of dominant bacteria communities during composting.

2. Materials and Methods

2.1. Materials

The raw pig manure suitable for composting was taken from Dongtian Pingchen Breeding Co., Ltd., Fujian Province, China, and had an initial carbon and nitrogen content of 30.5% and 3.0% (*w/w*), respectively, resulting in a C/N ratio of 10.2. Sawdust with a carbon and nitrogen content of 58.4% and 0.3% (*w/w*), respectively (C/N ratio of 224.6), was taken from Huanneng Timber Co., Ltd., Quanzhou, China, and was added to adjust the carbon composition of the pig manure. Both the pig manure and sawdust were crushed and sieved to pass through a 20-mesh screen for experiments.

The tea used for G-*n*Fe synthesis was Tieguanyin tea, provided free of charge by Anxi Tieguanyin planting base, Quanzhou, China. Special beef protein medium was used for counting the number of colony-forming units (CFU), where the product execution standard was GB/T 4789.28. Cabbage seeds for the germination studies were purchased from Kexiang Seed Co., Ltd., Quanzhou, China, where the product execution standard was GB16715.3-1999. All other reagents purchased from Aladdin Biochemical Technology Co., Ltd., Shanghai, China, were of analytical grade. The water used in all experiments was of high purity.

2.2. Synthesis of G-nFe

Tea extract was prepared by boiling dried tea (30 g) in high-purity water (500 mL) at 80 °C for 1 h. Thereafter, the prepared extracts were vacuum-filtered and immediately

sealed at $-4\,°C$ for subsequent use. Finally, we added an aliquot of tea extract to a 0.10 M $FeSO_4$ at a 2:1 ratio (v/v) and constantly stirred for 0.5 h in a nitrogen atmosphere to synthesize G-nFe (room temperature). The immediate appearance of a black color indicated the reduction of Fe^{2+} ions to Fe^o nanoparticles. The resulting black liquid suspension (G-nFe solution) was protected by nitrogen until being used in composting.

2.3. Characterization

To better understand the morphology and contact of the G-nFe and compost mixture, the dried samples (mixtures that were dried at 60 °C for 48 h) were crushed and sieved to pass through a 200-mesh screen (<0.0750 mm) prior to the analysis of the morphology using scanning electron microscopy (SEM) (JSM 7500 F, Japan). SEM mapping to measure the distribution of iron elements on the sample surface was carried out using scanning electron microscopy (SEM) (JSM 7500 F, Japan). The samples were affixed onto adhesive tapes supported on metallic disks and then covered with a thin, electric conductive gold film. Images were recorded at different magnifications at an operating voltage of 3 kV.

Fourier-transform infrared (FTIR) spectra of compost samples were recorded in the range of 648 to 4000 cm^{-1} with an average of nine scans for each measurement with a resolution of 2 cm^{-1} (FTIR Nicolet 5700, Thermo Corp., Waltham, MA, USA). Specimens suitable for FTIR measurement were prepared by mixing 1% (w/w) of the samples with 100 mg of KBr powder and pressing them into a sheer slice.

Volatile solids (VS): The compost samples (20 g) were dried in electrothermal draught drying cabinet at 105 °C for 24 h to obtain dried samples, and thereafter were crushed and sieved to pass through a 20-mesh screen (<0.850 mm) suitable for VS. The dried powdered sample (2.0 g) was accurately weighed into a dry crucible (accurate to 0.0001 g, so that two parallel experiments could be conducted), and calcinated in a muffle furnace at 600 °C for 4 h and then weighed after cooling. The VS and VS degradation rate (K) were calculated using the following equation:

$$VS = \frac{(b - d)}{(b - a)} \times 100\% \tag{1}$$

$$K = \frac{(VS_1 - VS_{15})}{VS_1} \times 100\% \tag{2}$$

where a (g) is the weight of the crucible after drying, b (g) is the weight of the crucible and sample before calcination, d (g) is the weight of the crucible and sample after calcination, and VS_1 and VS_{15} are the values of compost on days 1 and 15, respectively.

Analysis of compost extract: Sample mixtures (5 g) were mixed in high-purity water at a weight ratio of 1:10 and oscillated on a stable-temperature horizontal shaking bath for 2 h at 150 r/min before being centrifuged for 25 min (5000 r/min). The resulting supernatant solution was transferred to a beaker (100 mL) without solid sediment for further pH, oxidation-reduction potential (ORP), germination index (GI), and colony-forming unit (CFU) analyses. The pH and ORP were measured using an S400-B pH/ORP meter manufactured by Mettler Toledo, Ohio, USA.

Germination index (GI): Aqueous compost extract (1:10 (w/w); 5 mL) was transferred into a 9 cm diameter sterile culture dish with two qualitative filter papers. To each culture dish, 20 cabbage seeds were evenly spaced on the surface of the filter papers, which were then cultivated on a digital biochemical incubator at 30 °C for 48 h. The germination rate (P_e) and total root length (L_e) of the experiment seeds, together with the germination rate (P_c) and total root length (L_c) (root length measured with a ruler) of the control experimental seeds, were measured and the GI calculated as follows:

$$GI = (P_e \times L_e)/(P_c \times L_c) \times 100\% \tag{3}$$

Colony-forming units (CFU): The aqueous compost extract (1:10 (w/w)) was initially filtered through a disposable 0.45 μm mixed fiber microporous membrane and then diluted 10, 100, and 1000 times with distilled water. An aliquot of each individual diluent (1 mL) was transferred to a sterile culture dish using a sterile pipette. Thereafter, beef protein medium (15 mL) was added to every culture dish and rotated gently so that the diluents were thoroughly incorporated into the mixture. The culture dishes were then inverted and incubated at 30 °C for 24 h (i.e., three parallel experiments). After incubation, the number of colonies in each culture dish was counted and multiplied by the dilution factor to obtain the original compost extract's CFU. The disinfection and colony counted involved in the experiment were carried out in accordance with the national environmental protection standard No. HJ 1000–2018 of China.

DNA extraction and MiSeq sequencing of composting bacteria: Genomic DNA was extracted from the composted samples using the PowerSoil kit (Majorbio Laboratory, Shanghai, China) following the manufacturer's instructions. The DNA extracts were pooled and kept at −80 °C until analysis. The V3-V4 region of the bacteria 16S ribosomal RNA gene from each sample was subjected to polymerase chain reaction (PCR) amplification using universal primer 338F (5′-ACTCCTACGGGAGGCAGCAG-3′) and 806R (5′-GGACTACHVGGGT-WTCTAAT-3′) (Applied Biosystems, Foster City, CA, USA). Each sample was analyzed in triplicate. After purification, the Illumina MiSeq platform (Shanghai Majorbio Biopharm) was used for sequencing.

2.4. Thermophilic Aerobic Composting

Composting was conducted at a constant temperature of 55 °C and an intermittent oxygen supply. The thermophilic aerobic composting system consisted of six composting reactors (each with an effective volume of 3.5 L), where each reactor was equipped with a separate air distribution system and an oxygen generator (Figure 1A). After loading the reactor with the sample for testing, the experiment was initiated by placing the reactors in an incubator for cultivation (Figure 1A). The specific operation process of the composting system is included Figure 1B–D, showing the air blast, material deploy, and the culture of the composting process.
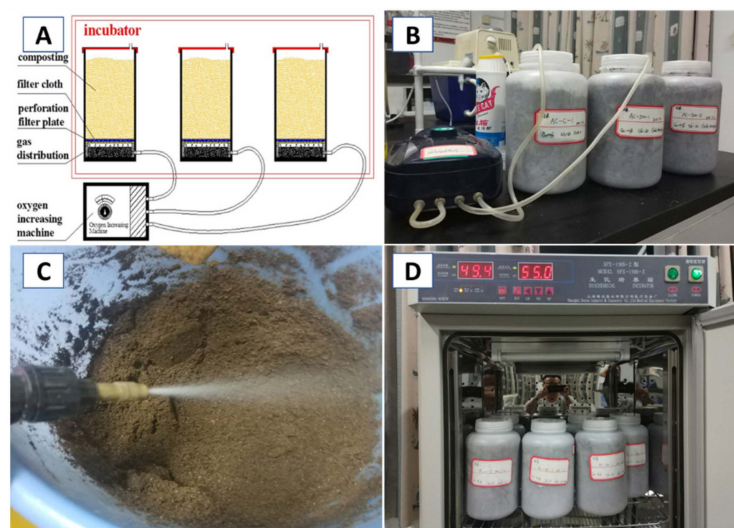

Figure 1. TAC composting system and some operation processes: (**A**) schematic diagram, (**B**) air blast, (**C**) material deploy, (**D**) culture.

A laboratory-scale thermophilic aerobic composting process was employed for three sets of batch experiments: (1) AC-C (control—aerobic compost with no added G-nFe solution); (2) AC-200 (the amount of G-nFe solution added to the compost was 200 mL/kg, in which the dry weight of the effective G-nFe particles was 0.13 g); and (3) AC-500 (the

amount of G-*n*Fe solution added to the compost was 500 mL/kg, in which the dry weight of the effective G-*n*Fe particles was 0.33 g). The pig manure and sawdust were initially combined to form the foundation composting pile (FCP) and controlled the C/N of FCP to 20 by adjusting the percentage of sawdust added. The compost was well homogenized using a wooden spade, and a 55% (*w/w*) moisture content was maintained by adding high-purity water. Every batch experiment was conducted in duplicate. The detailed experimental design is summarized in Table 1.

Table 1. Detailed experimental design of the composting experiments.

Test	FCP	G-*n*Fe (v/d w)	Aeration (Times/Day)	Aeration Time	Stirring Frequency /Artificial
AC-C	Yes	None added	5 times/day	5 min/times	5 times/day
AC-200	Yes	200 mL/kg	5 times/day	5 min/times	5 times/day
AC-500	Yes	500 mL/kg	5 times/day	5 min/times	5 times/day

Note: distribution of aeration time was every 4.8 h.

On days 1, 3, 5, 7, 10, and 15, samples were taken from multiple points throughout the compost and mixed together to obtain a composite sample for subsequent analysis. The further treatment and analysis methods of the samples are described in Section 2.3.

2.5. Statistical Analysis

After the DNA extraction and MiSeq sequencing of the composting bacteria, followed by bioinformatics analysis, Usearch (version 7.0 http://drive5.com/usearch/, accessed on 22 April 2019) was used to cluster the sequence data into operational taxonomic units (OTUs) via the SILVA database (Release128 http://www.arb-silva.de, accessed on 22 April 2019) according to 97% similarity. A number of different richness and diversity indices (e.g., abundance-based coverage estimator (ACE), Chao 1, Simpson, and Shannon) were calculated. The similarity and diversity of the bacterial communities during composting were measured by principal coordinates analysis (PCA) and nonmetric multidimensional scaling (NMDS). The relative abundance of the dominant bacteria community was analyzed after the taxonomic analysis.

3. Results and Discussion

3.1. Characterization of the G-nFe and Compost Mixture

As shown in Figure 2C,D, G-*n*Fe partially agglomerates and adheres to the compost after fully stirring and mixing with the compost. Compared with the compost with added G-*n*Fe (Figure 2A,B), the control experiment showed a relatively flat microscopic morphology. However, according to the SEM mapping analysis (Figure 2E,F), most iron elements were evenly distributed throughout the compost due to agitation. The uniform distribution ensures that the nanoparticles can fully contact with the compost, while partial agglomeration is helpful for the long-term effect of iron nanoparticles during composting. The control experiments (Figure 2C,D) also showed uniformly distributed and small amounts of iron, mainly from pig manure.

The same synthesized G-*n*Fe applied here had previously been used to investigate the passivation of Cd in compost and had already been characterized by both SEM and XPS. The nanoparticles used were quasi-spherical in shape with diameters ranging from 20 to 80 nm. The surface chemical compositions of G-*n*Fe were mainly composed of FeOOH, Fe_2O_3, FeO, and a small amount of zero-valent iron [21]. The surface chemical compositions of G-*n*Fe are important, because most studies agree that it is the surface composition that largely gives materials the ability to influence the physiochemical properties such as the pH, ORP, and microbial growth in composts.
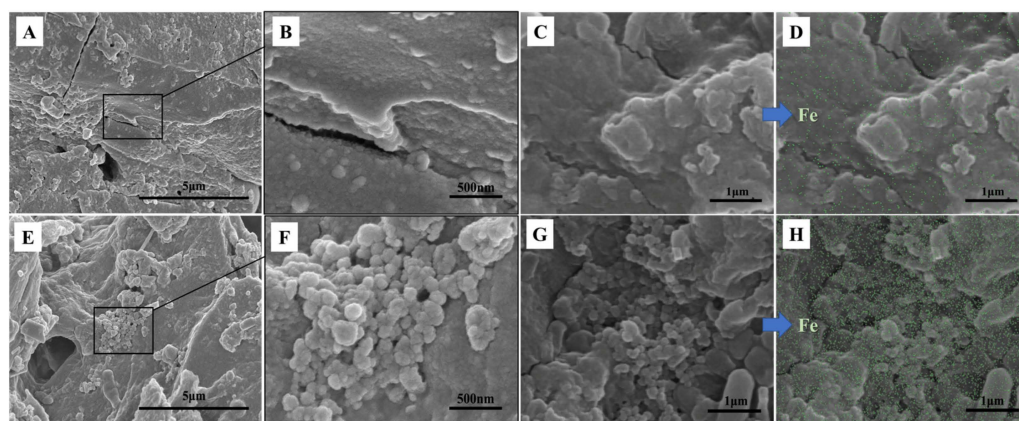
Figure 2. Characterization of the G-*n*Fe and compost mixture. (**A,B**) Control—aerobic compost at different magnification, (**C,D**) SEM mapping analysis of iron elements in control—aerobic compost, (**E,F**) compost with added G-*n*Fe at different magnifications, (**G,H**) SEM mapping analysis of compost with added G-*n*Fe.

3.2. Temporal Changes in pH, ORP, VS, and FTIR during Composting

Composting bacteria generally grow well under slightly acidic conditions, which can thus help to improve compost maturity. While the pH of livestock manure compost can vary over a wide range (from 3 to 11), the optimum pH is generally considered to be between 5.5 and 8 [22]. During this experiment, the pH varied through two stages: (1) an initial drop to a minimum, followed by (2) a uniform increase to a relatively high pH (Figure 3A). The initial rapid drop in pH was a consequence of the increased activity of acid-forming bacteria at the beginning of the composting process, which rapidly break down complex carbonaceous material to form organic acid intermediates. The subsequent rapid increase in the composting pH was mainly due to the decomposition of these organic acid intermediates and the conversion reaction of complex nitrogen-containing compounds to ammonia. The addition of G-*n*Fe significantly reduced the pH of the composting system, especially at the 200 mL/kg G-*n*Fe treatment. The lower pH indicated better acidic fermentation, which was advantageous as this favored significantly more organic matter degradation [23]. Both AC-200 and AC-500 showed lower pH levels over the whole composting cycle than the control experiment, especially AC-200. The difference was greatest on day 5, when the compost was at its most fermenting. This was attributed to G-*n*Fe promoting the growth of acid-forming bacteria during composting, a hypothesis that was supported by a later genus-level analysis of the dominant bacteria in the compost.

In addition to pH, the oxygen concentration of compost is another of the main factors influencing the oxidation-reduction potential (ORP) [24]. The ORP in the experiments varied through two distinct stages: (1) an initial drop to a low ORP, followed by (2) a rapid increase to its maximum level and then maintained at a relatively high level (Figure 3B). In the early stages of the experiment, the decrease in ORP was mainly attributed to the rapid proliferation of composting bacteria, which resulted in a relatively low oxygen concentration. Thereafter, with the increase in the oxygen concentration and the continuous accumulation of oxidizing substances, the ORP began to increase rapidly. The addition of G-*n*Fe reduced the ORP in the first five days, with the reduction in ORP being positively correlated with the G-*n*Fe dose. This was because the first five days corresponded to a logarithmic growth period of TAC bacteria, where a large amount of oxygen was used by rapidly growing composting bacteria, leading indirectly to the observed decrease in ORP. The addition of G-*n*Fe was thought to participate in two competing influences; while the G-*n*Fe directly promoted the decline in ORP via its innate reductive capacity, it could also promote the growth of compost bacteria indirectly, resulting in more oxygen being consumed (Figure 4).
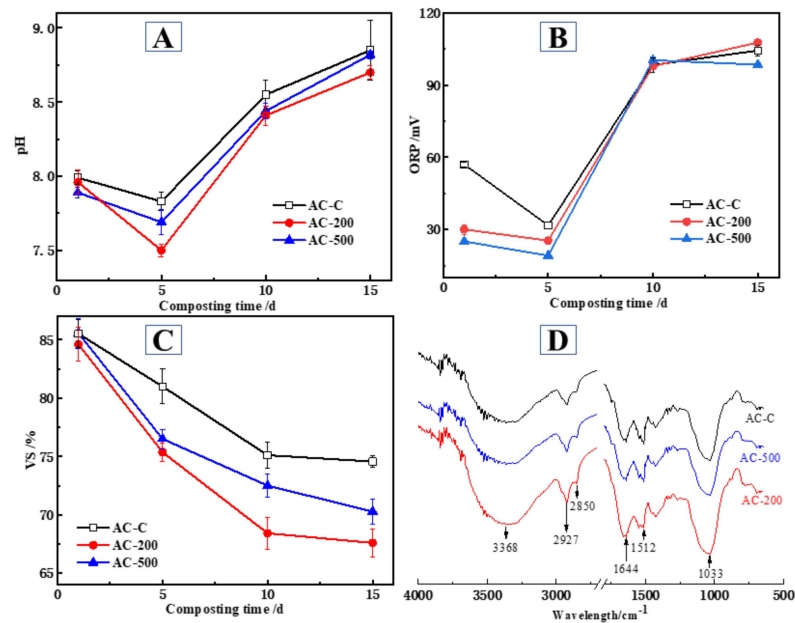
Figure 3. Temporal variation in pH (**A**), ORP (**B**), VS, (**C**) and FTIR spectra of the three final composting products (**D**).
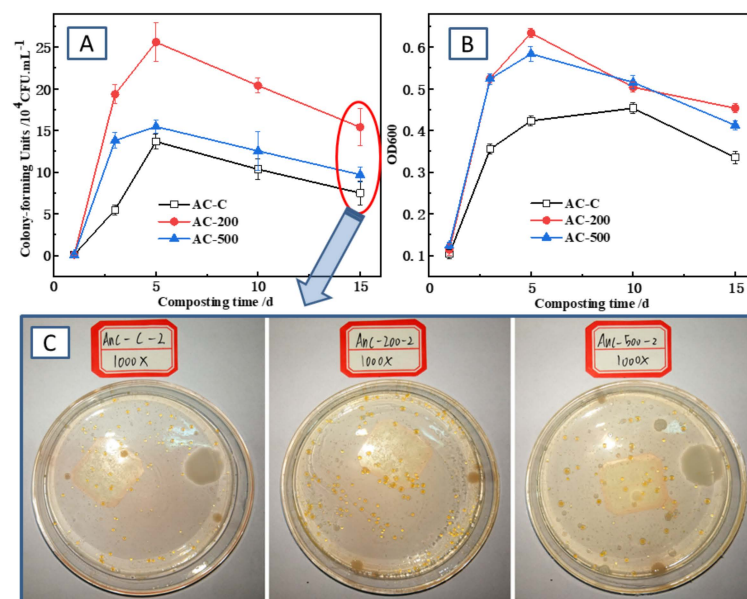

Figure 4. Temporal variation in CFU (**A**), OD600 (**B**) during composting, and colony growth on day 15 (**C**).

It is generally believed that the decrease in volatile solids (VS) to a relatively stable value during composting is an important sign that the compost is approaching maturity. Compost maturity is an important consideration, since the use of immature compost as a fertilizer can lead to heat injury of the seedlings and roots [13]. Ideally, VS degradation during composting should be between 17% and 53%, but in practice, the exact degradation percentage is largely related to the type of materials initially used. For example, when materials that are difficult to biodegrade are used, the amount of degradation may well be <10% [25]. Since the main material used in this experiment was sawdust, which is largely composed of poorly degradable lignin, a very high VS was not expected. As shown in Figure 3C, VS degradation rapidly increased to a high level within the first 3 days, before leveling off after the tenth day. The addition of G-*n*Fe significantly improved the

VS degradation throughout the composting cycle. When the concentration of G-nFe was 200 mL/kg, the VS degradation reached a maximum of 20.8%, which was 1.28 times that of the control experiment (16.2%). The difference in the degradation rate increased with the change in the composting time, which was related to the promotion effect of G-*n*Fe on the growth of dominant bacteria. The degradation of VS was mainly due to the microbial degradation of the organic matter in the compost, and when the VS remained stable, the compost was considered to be mature. The positive changes in VS following the addition of G-*n*Fe further confirmed that G-*n*Fe had a positive effect on the growth of compost bacteria and the maturing of the compost. The SEM mapping analysis (Figure 2) showed the uniform load of G-*n*Fe nanoparticles on the compost surface, while XPS revealed that the surface chemical compositions contained FeOOH, Fe_2O_3, FeO, and zero-valent iron [21], which were the main reasons why adequate G-*n*Fe could promote the VS degradation.

FTIR is a useful tool to quickly characterize any changes occurring in the organic groups of compost samples. Irrespective of the treatment, the FTIR spectra of the final compost products were basically the same (Figure 3D), indicating that the addition of G-*n*Fe resulted in no significant changes in the compost composition. For all spectra, broad bands near 3368 cm^{-1} corresponded to the O–H stretching of hydroxyl groups from phenol and alcohol and/or from carboxylic groups, as well as amide and amine N–H stretching [26]. Another broad and intense band in the region 1660–1600 cm^{-1} was attributed to the C=C vibrations of aromatic structures, possibly conjugated with C=O. Peaks in the 1080–1030 cm^{-1} range were attributed to the C–O stretching of polysaccharides. Other peaks at around 2927 and 2850 cm^{-1} were attributed to the symmetric and asymmetric stretching vibrations of aliphatic C–H bonds in the CH_3 and CH_2 groups. Together, these absorption peaks were consistent with the presence of significant amounts of humus in all composts. However, the addition of G-*n*Fe did result in some specific changes in the FTIR spectra of the composts; the addition of G-*n*Fe significantly increased the intensity of absorption peaks near 3368, 2927, 2850, 1644, and 1033 cm^{-1}, which were more obvious at 200 mL/kg G-*n*Fe. This indicated that G-*n*Fe promoted the generation of compost humus, a finding that is consistent with the previous conclusion that AC-200 promotes compost maturity.

3.3. Temporal Changes in OD600 and CFU during Composting

Changes in the CFU during composting reflects the changes in the proliferation of bacteria. OD600 was used to accurately determine the density of the bacterial cells in the culture medium, which is the standard method for tracking microbial growth in liquid cultures [27]. The combined analysis of these two indices was considered a good reflection of the changes in the microorganisms' growth during composting. As shown in Figure 4A, the CFU went through three stages in these experiments: (1) an initial rapid rise to its maximum, (2) maintenance at a high level for an extended period, and (3) a gradual decline to its minimum. The amount of CFU was very small when composting began because the bacteria were still in an adaptation stage. Thereafter, under the influence of increasing oxygen and temperature, the bacteria began to enter a rapid logarithmic growth phase and the bacterial numbers increased. However, eventually, as the organic matter was consumed and degraded, the compost tended to maturate, and the CFU slowly dropped to a much lower level. For both treatments, the addition of G-*n*Fe increased CFU (Figure 4A), with the highest number of CFU occurring for 200 mL/kg G-*n*Fe. The temporal changes in OD600 mirrored the variations observed in the CFU (Figure 4B). The observed changes in the CFU and OD600 further supported the hypothesis that G-nFe promoted the growth of bacteria during composting, which reached its apogee when the concentration of G-nFe was 200 mL/kg. As shown in Figure 4C, when 200 mL/kg of G-nFe was added, the number of colonies was significantly larger than that in either the AC-C or the AC-500 treatments. Some previous studies have proposed that iron nanoparticles can disrupt cell membranes, entering bacterial cells in high concentrations, thereby causing adverse outcomes [28,29]. However, provided the concentration of nFe was sufficiently low to minimize any toxicity,

any H2 produced through iron corrosion could be used as an electron source by some compost bacteria to promote growth [20]. Another advantage of nFe, not commonly considered in relation to composting, is its ability to reduce contaminant toxicity. Thus, in this experiment, G-*n*Fe may have effectively reduced the activity of the heavy metals and degraded some organic pollutants in pig manure, resulting in overall reduced compost toxicity and indirectly leading to the increased growth of compost bacteria.

3.4. Temporal Changes in GI during Composting

Chanyasak et al. [30] posited that phytotoxicity is an obvious biological indicator of compost maturity, because mature composts progress through periods of high compound degradation to effectively eliminate any initial phytotoxicity. Plant toxicity is usually measured by simple seed germination experiments, where the germination index (GI) can not only detect compost phytotoxicity, but can also be used to monitor the progress of toxicity reduction towards compost maturity as the composting proceeds [31].

As shown in Figure 5, during composting, the GI went through two distinct stages: (1) a rapid decrease to a minimum, and followed by (2) a significant rise to a maximum and maintained at a relatively high GI. After adding G-*n*Fe, the GI significantly decreased in the initial 7 days of composting, mainly due to a large number of organics such as proteins that were decomposed into organic acids, aldehydes, and ammonia, which inhibited the seeds' germination. As the composting progressed, organic acids and aldehydes were slowly further decomposed, and ammonia gas was either slowly released into the air or converted into nontoxic ionic forms. Consequently, the GI started to increase as the compost slowly approached maturity. The addition of G-*n*Fe resulted in an increase in GI throughout the composting period, which was more pronounced when the concentration of G-*n*Fe was 200 mL/kg. Previous research has shown that neither fresh nor aged *n*ZVI revealed any visible toxic effects on rice seedlings or plant growth at low concentrations, and did not cause excessive lipid peroxidation. Even at higher concentrations (1000 mg/kg (w/w%) in soil), the phytotoxicity of the iron nanoparticles was limited. [32] Researchers currently attribute the toxicity of pure *n*ZVI to increasing levels of reactive oxygen species and their ability to induce iron deficiency in seedlings [32,33]. In this experiment, the amount of G-*n*Fe added was relatively small, so the any phytotoxicity produced was likely to be extremely small compared to the beneficial aspects associated with the promotion of beneficial composting processes and the reduction in compost toxicity.
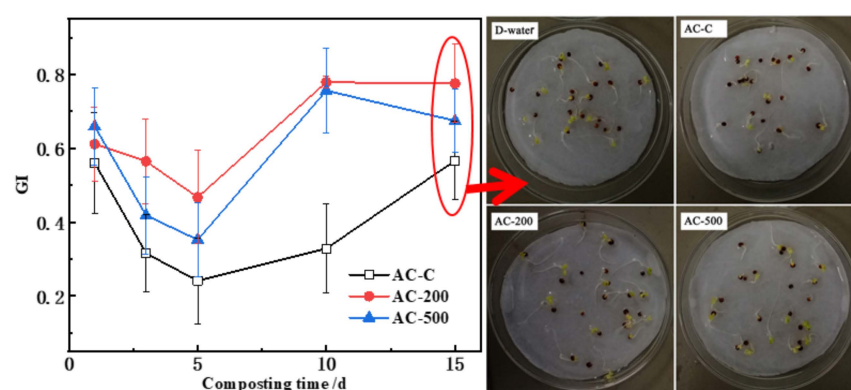

Figure 5. Temporal variation in GI during composting and pictures of final seed germination for the three treatments and the control at day 15.

3.5. Analysis of Bacteriological Changes during Composting

3.5.1. OTUs and Alpha Diversity of Compost Bacterial

Venn diagrams (Figure 6A–C) revealed that the OTUs of all three composting treatments were reduced. This analysis indicated that while the dominant bacteria increased during the composting process, other bacteria decreased and the relative number of microbial populations also gradually decreased. The common OTUs were 149, 157, and 147,

respectively, indicating that most of the dominant bacteria were retained and were most prevalent when G-*n*Fe was added at 200 mL/kg. For all three compost treatments, the common OTUs were 128 on the 15th day of composting (Figure 6D), indicating that the addition of G-*n*Fe did not significantly change the dominant bacteria in the compost. This was important, because minimal disturbance of bacterial communities is desired when the compost is destined for subsequent soil applications. The OTUs of AC-200 reached a maximum of 207, meaning that 200 mL/kg G-*n*Fe promoted the bacterial population the most at the end of composting.
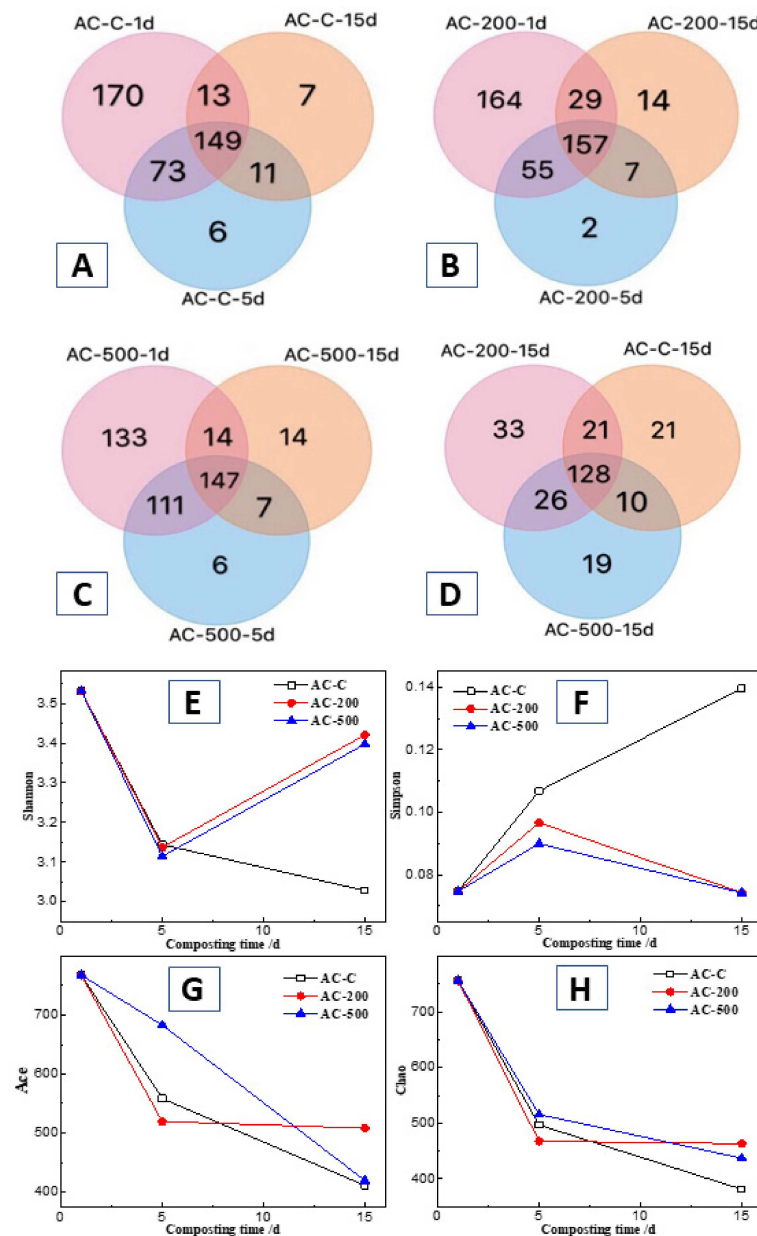

Figure 6. Venn diagram of OTUs during composting for treatments AC-C (**A**), AC-200 (**B**), and AC-500 (**C**), a comparison of the three treatments at day 15 (**D**), and Alpha diversity analysis using the Shannon (**E**), Simpson (**F**), Ace (**G**), and Chao (**H**) indices.

Alpha diversity is an indicator of population abundance and uniformity, and is commonly applied to quantify the diversity within a given region or ecosystem. The Shannon index was positively related to the bacterial population diversity in the compost, but the Simpson index was negatively related. The Ace and Chao indices were related to the abundance of bacterial communities in the compost. Temporal changes in the four common

diversity indices are shown in Figure 6E–H. In the control experiment, the decrease in the Shannon index and the increase in the Simpson index indicated that the diversity of the bacterial population decreased during composting. Likewise, the decreases in both the Ace and Chao indices indicated that the richness of the bacterial communities decreased during composting.

When G-*n*Fe was added, the bacterial diversity increased in the later composting period, as indicated by an increase in the Shannon index and a decrease in the Simpson index. This was contrary to the results observed in the control experiment. The Ace and Chao indices also showed that the addition of G-*n*Fe promoted increased bacterial community diversity. Thus, the bacterial diversity and community richness were best in the later stages of composting when 200 mL/kg G-*n*Fe had been added.

3.5.2. Temporal Variation in the Abundance of Dominant Bacterial Communities

The relative abundance of the top 10 dominant bacteria during composting were analyzed. As seen from the relative abundance on day 1 (Figure 7A), the dominant bacteria in the initial pig manure were *Clostridium sensu stricto 1*, *Bacillus*, *Terrisporobacter*, *Turicibacter*, *Romboutsia*, *Corynebacterium 1*, and *Streptococcus*, all of which are commonly found in the intestines of livestock [34,35]. However, due to the high temperatures experienced during composting, the relative abundance of these bacteria changed over time.
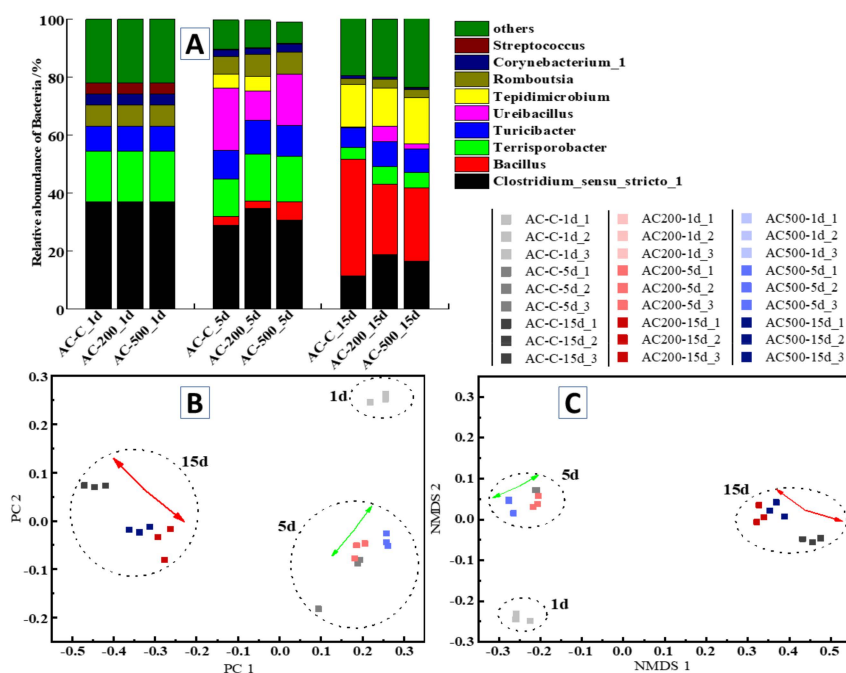

Figure 7. Change in relative abundance of bacteria (**A**) and similarity analysis of bacterial communities during composting at the genus level via PCA analysis (**B**) and NMDS analysis (**C**).

Clostridium sensu stricto 1 was the dominant type of acid-forming bacteria, known to mainly produce acetic acid, butyric acid, and a small amount of propionic acid [36]. The decrease in its relative abundance was due to the continuous decrease in biodegradable organic matter (the main food source for bacteria) in the compost, which led to an increase in pH and affected the compost maturity [23]. The addition of G-*n*Fe increased the relative abundance of *Clostridium sensu stricto 1* in the compost, which reached 34.5% and 18.6% at day 5 and day 15, respectively. When the addition of G-*n*Fe was 200 mL/kg, the abundance of *Clostridium sensu stricto 1* led to increased compost maturity [23,37]. This was consistent with the analysis of VS, which showed the highest VS degradation rate for AC-200. *Turicibacter* was another acid-forming bacterium present in the compost. When the addition of G-*n*Fe was 200 mL/kg, the relative abundance of *Turicibacter* was 11.5 and 18.6%

on the 5th and 15th days, respectively, which was significantly higher than the abundances observed in either the AC-C or AC-500 treatments. The promotion effect of added G-*n*Fe on acid-forming bacteria directly demonstrated the inhibitory effect of G-*n*Fe on the pH of compost (Figure 3A).

Streptococcus, *Corynebacterium 1* and *Terrisporobacter* are three common intestinal pig pathogens that can cause a large number of human and animal diseases [38]. Thus, it was beneficial that their relative abundance gradually decreased during composting due to the high temperature experienced during composting, which can kill most pathogenic bacteria, and which was thus conducive to ensuring the production of high-quality compost [39]. However, of some concern was that even after 15 days of high-temperature composting, these three intestinal pathogens were still relatively abundant. This aspect needs further research as the composting period may need to be increased to completely remove such pathogens.

The presence of *Bacillus* is usually related to high-temperature degradation resulting in phosphorus dephosphorization during composting, and is thus conducive to promoting composting maturity [40]. It was encouraging that the relative abundance of *Bacillus* increased during composting, and while the relative abundance of Bacillus in AC-500 only reached 6.3% on day 5, this increased to 25.3% on day 15. Of some concern was the observation that G-*n*Fe had a slight inhibitory effect on Bacillus late in the composting process (Figure 7).

Ureibacillus is a thermophilic bacterium capable of degrading nitrogen-containing organic matter to produce urea and ammonia, where an increase in its mass growth usually indicates that composting has moved from acidic to alkaline fermentation [41]. On day 5 of composting, the addition of G-*n*Fe significantly reduced the relative abundance of *Ureibacillus*, with AC-200 having the lowest abundance amongst the treatments, which is another reason why G-*n*Fe reduced pH (Figure 3A), and extended the acidic fermentation time of the composting. This is advantageous because, usually, the longer the acid fermentation time, the more thorough the organic degradation and the better the compost maturity.

Overall, the addition of G-*n*Fe increased the relative abundance of the acid-forming bacteria *Clostridium sensu stricto 1* and *Turicibacter* throughout the whole composting period and inhibited the relative abundance of the ammonia-forming bacterium *Ureibacillus*, which was most obvious when the addition of G-*n*Fe was 200 mL/kg. These changes indicated that the acidic fermentation time of the composting had been prolonged and, as a result, the compost maturity should be increased.

3.5.3. Similarities and Differences between Bacterial Communities

The PCA analysis at the genus level (Figure 7B) showed that the composting time was the main factor leading to differences in the bacterial community composition. The longer the composting time, the more obvious the effect of G-*n*Fe on the community differences in the composting bacteria, which was the greatest at 15 days and when the addition of G-*n*Fe was 200 mL/kg.

The NMDS analysis at the genus level (Figure 7C) was also considered reliable, since all of the data from the NMDS were below 0.1 and were also consistent with the PCA analysis. Again, the composting time was the main factor leading to differences in the bacterial species, where the difference became larger as the composting progressed. As with the PCA, the addition of G-*n*Fe increased the species diversity of the composting bacteria, where the largest diversity was observed when the concentration of G-*n*Fe was 200 mL/kg.

4. Conclusions

The effect of green synthesized iron nanoparticles on the aerobic composting process of pig manure was investigated. The addition of G-*n*Fe decreased both pH and ORP and promoted the growth of bacteria in the early stages of composting, especially when the amount of G-*n*Fe was 200 mL/kg. At this concentration of G-*n*Fe, the GI of the

compost was also the best, indicating that the phytotoxicity of the compost was at its lowest, the humification was highest, and VS degradation reached the highest level (20.8%). Furthermore, during composting, the addition of G-*n*Fe improved both bacterial diversity and community richness and increased the differences among the bacterial communities. Specifically, G-*n*Fe increased the relative abundance of common acid-forming bacteria such as *Clostridium sensu stricto 1* and *Turicibacter* over the whole composting cycle and inhibited the relative abundance of ammonia-forming bacteria such as *Ureibacillus*. This indicated that adding G-*n*Fe has a positive effect on composting promotion and nitrogen retention. The effects on the bacterial communities were most pronounced when the addition of G-*n*Fe was 200 mL/kg. These results suggested that G-*n*Fe extended the acidic fermentation time during composting and increased compost maturity. Thus, considering the modest amount of G-*n*Fe applied here and its relatively low toxicity, G-*n*Fe could have significant beneficial impacts on creating better quality composts.

References

1. Stefaniuk, M.; Oleszczuk, P.; Yong, S.O. Review on nano zerovalent iron (nZVI): From synthesis to environmental applications. *Chem. Eng. J.* **2016**, *287*, 618–632. [CrossRef]
2. Yi, Y.; Tu, G.; Tsang, P.; Xiao, S.; Fang, Z. Green synthesis of iron-based nanoparticles from extracts of Nephrolepis auriculata and applications for Cr(VI) removal. *Mater. Lett.* **2019**, *234*, 388–391. [CrossRef]
3. Khatami, M.; Alijani, H.; Fakheri, B.; Mobasseri, M.; Heydarpour, M.; Farahani, Z.; Khan, A. Super-paramagnetic iron oxide nanoparticles (SPIONs): Greener synthesis using Stevia plant and evaluation of its antioxidant properties. *J. Clean. Prod.* **2019**, *208*, 1171–1177. [CrossRef]
4. Luo, F.; Yang, D.; Chen, Z.; Megharaj, M.; Naidu, R. The mechanism for degrading Orange II based on adsorption and reduction by ion-based nanoparticles synthesized by grape leaf extract. *J. Hazard. Mater.* **2015**, *296*, 37–45. [CrossRef]
5. Fang, L.; Chen, Z.; Megharaj, M.; Naidu, R. Simultaneous removal of trichloroethylene and hexavalent chromium by green synthesized agarose-Fe nanoparticles hydrogel. *Chem. Eng. J.* **2016**, *294*, 290–297.
6. Christina, L. Pharmaceuticals. China's lakes of pig manure spawn antibiotic resistance. *Sci. Total Environ.* **2015**, *347*, 704.
7. Pan, X.; Qiang, Z.; Ben, W.; Chen, M. Residual veterinary antibiotics in swine manure from concentrated animal feeding operations in Shandong Province, China. *Chemosphere* **2011**, *84*, 695–700. [CrossRef]
8. Zitnick, K.K.; Shappell, N.W.; Hakk, H.; Desutter, T.M.; Khan, E.; Casey, F.X.M. Effects of liquid swine manure on dissipation of 17β-estradiol in soil. *J. Hazard. Mater.* **2011**, *186*, 1111–1117. [CrossRef]
9. Li, L.; Xu, Z.; Wu, J.; Tian, G. Bioaccumulation of heavy metals in the earthworm Eisenia fetida in relation to bioavailable metal concentrations in pig manure. *Bioresour. Technol.* **2010**, *101*, 3430–3436. [CrossRef]
10. Ziemer, C.J.; Bonner, J.M.; Cole, D.; Vinjé, J.; Constantini, V.; Goyal, S.; Gramer, M.; Mackie, R.; Meng, X.J.; Myers, G. Fate and transport of zoonotic, bacterial, viral, and parasitic pathogens during swine manure treatment, storage, and land application. *J. Anim. Sci.* **2010**, *88*, E84–E94. [CrossRef]
11. Fang, H.; Han, L.; Zhang, H.; Long, Z.; Cai, L.; Yu, Y. Dissemination of antibiotic resistance genes and human pathogenic bacteria from a pig feedlot to the surrounding stream and agricultural soils. *J. Hazard. Mater.* **2018**, *357*, 53. [CrossRef] [PubMed]
12. Kang, Y.; Hao, Y.; Shen, M.; Zhao, Q.; Li, Q.; Hu, J. Impacts of supplementing chemical fertilizers with organic fertilizers manufactured using pig manure as a substrate on the spread of tetracycline resistance genes in soil. *Ecotoxicol. Environ. Saf.* **2016**, *130*, 279–288. [CrossRef] [PubMed]
13. Wan, N.; Hwang, E.Y.; Cheong, J.G.; Choi, J.Y. A Comparative Evaluation of Maturity Parameters for Food Waste Composting. *Compos. Sci. Util.* **1999**, *7*, 55–62.

14. Huang, G.F.; Wong, J.W.C.; Wu, Q.T.; Nagar, B.B. Effect of C/N on composting of pig manure with sawdust. *Waste Manag.* **2004**, *24*, 805–813. [CrossRef] [PubMed]

15. Wu, X.; Wei, Y.; Zheng, J.; Xin, Z.; Zhong, W. The behavior of tetracyclines and their degradation products during swine manure composting. *Bioresour. Technol.* **2011**, *102*, 5924–5931. [CrossRef]

16. Wang, Q.; Li, R.; Cai, H.; Awasthi, M.K.; Zhang, Z.; Wang, J.J.; Ali, A.; Amanullah, M. Improving pig manure composting efficiency employing Ca-bentonite. *Ecol. Eng.* **2016**, *87*, 157–161. [CrossRef]

17. Ran, X.; Awasthi, M.K.; Li, R.; Park, J.; Pensky, S.M.; Quan, W.; Wang, J.J.; Zhang, Z. Recent developments in biochar utilization as an additive in organic solid waste composting: A review. *Bioresour. Technol.* **2017**, *246*, 203–213.

18. Ye, K.; Yan, Z.; Chen, Z.; Megharaj, M.; Naidu, R. Impact of Fe and Ni/Fe nanoparticles on biodegradation of phenol by the strain Bacillus fusiformis (BFN) at various pH values: Biomass, bioenergy, biowastes, conversion technologies, biotransformations, production technologies. *Bioresour. Technol.* **2013**, *136*, 588–594.

19. Jiang, C.; Liu, Y.; Chen, Z.; Megharaj, M.; Naidu, R. Impact of iron-based nanoparticles on microbial denitrification by Paracoccus sp. strain YF1. *Aquat. Toxicol.* **2013**, *142–143*, 329–335. [CrossRef]

20. Liu, Y.; Li, S.; Chen, Z.; Megharaj, M.; Naidu, R. Influence of zero-valent iron nanoparticles on nitrate removal by *Paracoccus* sp. *Chemosphere* **2014**, *108*, 426–432. [CrossRef]

21. Yang, W.-q.; Zhuo, Q.; Chen, Q.; Chen, Z. Effect of iron nanoparticles on passivation of cadmium in the pig manure aerobic composting process. *Sci. Total Environ.* **2019**, *690*, 900–910. [CrossRef] [PubMed]

22. Bertoldi, M.D.; Vallini, G.; Pera, A. The biology of composting: A review. *Waste Manag. Res.* **1983**, *1*, 157–176. [CrossRef]

23. Jiang, J.; Huang, H.; Huang, Y.; Liu, X.; Liu, D. Relationship between maturity and microbial communities during pig manure composting by phospholipid fatty acid (PLFA) and correlation analysis. *J. Environ. Manag.* **2018**, *206*, 532–539. [CrossRef] [PubMed]

24. Wang, K.; Yin, X.; Mao, H.; Chu, C.; Tian, Y. Changes in structure and function of fungal community in cow manure composting. *Bioresour. Technol.* **2018**, *255*, 123–130. [CrossRef] [PubMed]

25. Saludes, R.B.; Iwabuchi, K.; Kayanuma, A.; Shiga, T. Composting of dairy cattle manure using a thermophilic–mesophilic sequence. *Biosyst. Eng.* **2007**, *98*, 198–205. [CrossRef]

26. Baddi, G.A.; Hafidi, M.; Cegarra, J.; Alburquerque, J.A.; Gonzálvez, J.; Gilard, V.; Revel, J.C. Characterization of fulvic acids by elemental and spectroscopic (FTIR and 13 C-NMR) analyses during composting of olive mill wastes plus straw. *Bioresour. Technol.* **2004**, *93*, 285–290. [CrossRef]

27. Kothary, M.H.; Chase, T., Jr.; Macmillan, J.D. Levels of Aspergillus fumigatus in air and in compost at a sewage sludge composting site. *Environ. Pollut.* **1984**, *34*, 1–14. [CrossRef]

28. Changha, L.; Jee Yeon, K.; Won, I.L.; Nelson, K.L.; Jeyong, Y.; Sedlak, D.L. Bactericidal effect of zero-valent iron nanoparticles on *Escherichia coli*. *Environ. Sci. Technol.* **2008**, *42*, 4927–4933.

29. Wang, Z.; Lee, Y.-H.; Wu, B.; Horst, A.; Kang, Y.; Tang, Y.J.; Chen, D.-R. Anti-microbial activities of aerosolized transition metal oxide nanoparticles. *Chemosphere* **2010**, *80*, 525–529. [CrossRef]

30. Chanyasak, V.; Katayama, A.; Hirai, M.F.; Mori, S.; Kubota, H. Effects of compost maturity on growth of komatsuna (*brassica rapa* var. pervidis) in neubauer's pot. *Soil Sci. Plant Nutr.* **1983**, *29*, 239–250. [CrossRef]

31. Kato, K.; Miura, N. Effect of matured compost as a bulking and inoculating agent on the microbial community and maturity of cattle manure compost. *Bioresour. Technol.* **2008**, *99*, 3372–3380. [CrossRef] [PubMed]

32. Wang, J.; Fang, Z.; Cheng, W.; Tsang, P.E.; Zhao, D. Ageing decreases the phytotoxicity of zero-valent iron nanoparticles in soil cultivated with *Oryza sativa*. *Ecotoxicology* **2016**, *25*, 1202–1210. [CrossRef] [PubMed]

33. Foyer, C.H.; Shigeru, S. Understanding oxidative stress and antioxidant functions to enhance photosynthesis. *Plant Physiol.* **2011**, *155*, 93–100. [CrossRef] [PubMed]

34. Chen, Z.; Wang, Y.; Wen, Q. Effects of chlortetracycline on the fate of multi-antibiotic resistance genes and the microbial community during swine manure composting. *Environ. Pollut.* **2018**, *237*, 977–987. [CrossRef]

35. Snell-Castro, R.; Godon, J.-J.; Delgenès, J.-P.; Dabert, P. Characterisation of the microbial diversity in a pig manure storage pit using small subunit rDNA sequence analysis. *FEMS Microbiol. Ecol.* **2005**, *52*, 229–242. [CrossRef]

36. Yang, G.; Wang, J. Pretreatment of grass waste using combined ionizing radiation-acid treatment for enhancing fermentative hydrogen production. *Bioresour. Technol.* **2018**, *255*, 7–15. [CrossRef]

37. Tang, J.; Li, X.; Zhao, W.; Wang, Y.; Cui, P.; Zeng, R.J.; Yu, L.; Zhou, S. Electric field induces electron flow to simultaneously enhance the maturity of aerobic composting and mitigate greenhouse gas emissions. *Bioresour. Technol.* **2019**, *279*, 234–242. [CrossRef]

38. Zhang, R.; Gu, J.; Wang, X.; Li, Y.; Zhang, K.; Yin, Y.; Zhang, X. Contributions of the microbial community and environmental variables to antibiotic resistance genes during co-composting with swine manure and cotton stalks. *J. Hazard. Mater.* **2018**, *358*, 82–91. [CrossRef]

39. Bernal, M.P.; Sommer, S.G.; Chadwick, D.; Qing, C.; Guoxue, L.; Michel, F.C. Chapter Three—Current Approaches and Future Trends in Compost Quality Criteria for Agronomic, Environmental, and Human Health Benefits. In *Advances in Agronomy*; Sparks, D.L., Ed.; Academic Press: Cambridge, MA, USA, 2017; Volume 144, pp. 143–233.

40. Arif, M.S.; Riaz, M.; Shahzad, S.M.; Yasmeen, T.; Ali, S.; Akhtar, M.J. Phosphorus-Mobilizing Rhizobacterial Strain Bacillus cereus GS6 Improves Symbiotic Efficiency of Soybean on an Aridisol Amended with Phosphorus-Enriched Compost. *Pedosphere* **2017**, *27*, 1049–1061. [CrossRef]

41. Nakasaki, K.; Tran, L.T.H.; Idemoto, Y.; Abe, M.; Rollon, A.P. Comparison of organic matter degradation and microbial community during thermophilic composting of two different types of anaerobic sludge. *Bioresour. Technol.* **2009**, *100*, 676–682. [CrossRef]